Supporting Information

Ammonium enhances food waste fermentation to high-value optically active L-lactic acid

Wenjuan Zhang,[†] Xianbao Xu,[†] Pingfeng Yu,[‡] Pengxiao Zuo,[‡] Ya He,[‡] Hong Chen,[†] Yanan Liu,[†] Gang Xue,[†§] Xiang Li,[*†‡] and Pedro J.J Alvarez[‡]

[†] *College of Environmental Science and Engineering, State Environmental Protection Engineering Centre for Pollution Treatment and Control in Textile Industry, Donghua University, 2999 North Renmin Road, Shanghai 201620, China*

[‡] *Department of Civil and Environmental Engineering, Rice University, Houston, Texas 77005, United States*

[§] *Shanghai institute of pollution control and ecological security, 1239 Siping Road, Shanghai 200092, China*

*Corresponding author

E-mail: lix@dhu.edu.cn;

Tel: 86-21-67792538

Fax: 86-21-67792159

Supplementary data: 18 pages, 8 Tables, 15 Figures

Method of preliminary study

To evaluate the feasibility in long-term fermentation, FW and non-autoclaved WAS were mixed at a ratio of 6 g VSS/1 g VSS in the preliminary study, adding tap water to dilute final TCOD around 40 ± 1 g/L. The reactors were carried out with 1000 mL working volume and mechanically stirred at 120 rpm. Temperature was controlled using a water bath at mesophilic (35 ± 1°C) and the pH was intermittently adjusted to 9.0 ± 0.1 by adding sodium hydroxide (10 M) and hydrochloric acid (3 M) every 6 h. In the first run (R1), reactors were fed with 200 mL the same inoculum from seed reactor (SR) and 800 mL corresponding substrate mentioned above. Every 4 days, 200 mL of the fermentation mixture was retained and 800 mL of corresponding fresh substrate was fed. The repeated batch fermentation was operated in eight cycles for 32 days. Approximately 5-15 mL of dissolved samples were prepared by filtration through a cellulose acetate filter with pore size of 0.45 μm daily to analyze L- and D-LA. Sludge samples were collected after 3 days fermentation at the 4^{th} and 6^{th} cycle to analyze microbial community structure using 16S rRNA gene pyrosequencing.

Quantitation PCR (qPCR) of ammonia oxidation and denitrification related genes

Ammonia oxidation and denitrification related genes were detected by qPCR (LightCycler® 96, Roche Diagnostics GmbH, Mannheim, Germany). Each reaction was performed in a 20-μL volume containing 10 μL of FastStart Essential DNA Green Master (Roche Diagnostics GmbH, Mannheim, Germany), 2 μL each of forward and reverse primers (3 μmol/L), 1μL of template genomic DNA, and 5 μL of DNA-free water. For 16s rRNA (the primer 5'- AGGAAGGTGGGGATGAC -3', and 5'- CGGCTTTCTGGGATTGG -3'), the qPCR reactions were performed with a temperature program as follows: initial denaturing for 15 min at 95 °C, followed by 40 cycles of 10 s at 95 °C, annealing for 20 s at 57 °C and extending for 30 s at 72 °C. For *aomA* (the primer 5'- GAATATGTTCGCCTGATTG -3', and 5'- CAAAGTACCACCATACGCAG -3'), thermocycling began at 95 °C for 10 min followed by 40 cycles with a sequence of 95 °C for 15 s, 60 °C for 15 s, and 72°C for 15 s. For *nirS* (the primer 5'- TACCACCC(C/G)GA(A/G)CCGCGCGT -3', and 5'- GCCGCCGTC(A/G)TG(A/C/G)AGGAA -3'), the thermal cycling conditions applied 10 min at 95 °C, followed by 45 cycles at 95 °C for 15 s, 58 °C for 20 s, and 72°C for 30 s. For *narG* (the primer 5'- TAYGTSGGGCAGGARAAACTG

-3', and 5'- CGTAGAAGAAGCTGGTGCTGTT -3'), the thermal protocol consisted of 10 min at 95 °C, followed by 45 cycles at 95 °C for 30 s, 61 °C for 30 s, and 72°C for 20 s. All reactions were performed using three replicates per sample and contained the control reactions without template DNA. The copy number of total genes was calculated using a standard curve generated by using 10-fold serial dilutions of linearized plasmids containing the gene fragment as a template.

Electron balance calculation in Table S7.

The total number of electrons transferred N = *nM*, where *M* represents the number of moles, *n* represents the number of moles of electrons transferred in half reaction.

For NH_4^+-N, 15.3% of the utilized NH_4^+-N converted to NO_3^--N by ammonium oxidation process (*n*=8), and 31.0% converted to N_2 (*n*=3) based on ^{15}N isotope tracing in Figure S10. Therefore, the total number of electrons transferred based on the reagent NH_4^+-N:

$N(PyNH_4\text{-}R) = (300.3\text{-}168.8)/14 \times (31\%\times3+15.3\%\times8) = 20.23$ mM;

$N(Am\text{-}N) = (265.36\text{-}133.30)/14 \times (31\%\times3+15.3\%\times8) = 20.32$ mM.

For the product, NO_3^- (*n*=8) during $NH_4^+ \rightarrow NO_3^-$. The total number of electrons transferred:

$N(PyNH_4\text{-}R) = (34.8\text{-}0.11)/14 \times 8 = 19.82$ mM;

$N(Am\text{-}N) = (46.62\text{-}9.38)/14 \times 8 = 21.28$ mM.

For the reagent pyruvate during pyruvate→lactic acid (*n*=2). The total number of electrons transferred:

$N(PyNH_4\text{-}R) = (1441.1\text{-}25.8)/88/1000 \times 2 = 32.17$ mM.

For the product, lactate produced from pyruvate→lactic acid (*n*=2). The total number of electrons transferred:

$N(PyNH_4\text{-}R) = (957.41\text{-}0.35)/90/1000 \times 2 = 21.27$ mM.

$N(Am\text{-}N) = 22.95/90 \times 2 = 510.0$ mM.

Calculation in Figure 2. Each box plot shows minimum, first quartile, median, third quartile, and maximum values in Figure 2a~2f. Amount of ΔS_{COD} in Figure 2a and the rate of carbohydrate reduction in Figure 2d were described based on the absolute values in eight recycles. The rate of soluble carbohydrate reduction was the first order reaction rate constant based on the carbohydrate variations. Amount of the relative activities of enzymes in Figure 2b, 2c, 2e, and 2f were described based on the relative activity values in eight recycles. The maximum data of the relative activity of enzymes were set as 100.00, and the unit was %.

Table S1

Summary of the experimental fermentation parameters

Test No.	Figures and Tables	Fermenter	Mode	Volume (mL)	pH	Extra addition	Substrate
Test 1	Figure S2 and S7	Seed Reactor (SR)	Batch	1000	9.0 ± 0.1	--	Mixture of FW and WAS (TCOD = 40 g/L)
Test 2	Figure S1-S2	Preliminary study	Repeated batch	1000	9.0 ± 0.1	--	R1: 200 mL SR and 800 mL (Mixture of FW and WAS) R2 -R8: 200 mL (substrate from last Run) and 800 mL (Mixture of FW and WAS) (TCOD of FW and WAS mixture was 40 g/L)
Test 3 Ammonium dosage	Figure S3; and Table 1	0 mg/L	Batch	500	9.0 ± 0.1	-	100 mL SR and 400 mL FW (TCOD of FW was 40 g/L)
		100mg/L	Batch	500	9.0 ± 0.1	NH_4^+-N 100 mg/L	
		200 mg/L	Batch	500	9.0 ± 0.1	NH_4^+-N 200 mg/L	
		300 mg/L	Batch	500	9.0 ± 0.1	NH_4^+-N 300 mg/L	
		400 mg/L	Batch	500	9.0 ± 0.1	NH_4^+-N 400 mg/L	
		500 mg/L	Batch	500	9.0 ± 0.1	NH_4^+-N 500 mg/L	
		1000 mg/L	Batch	500	9.0 ± 0.1	NH_4^+-N 1000 mg/L	
Test 4	Figure 1-3, 4a, 6, 7; and Figure S4-S9, S11-S14; and Table S2-S6	Ctrl	Repeated batch	1000	9.0 ± 0.1	--	R1: 200 mL SR and 800 mL FW R2 -R8: 200 mL (substrate from last Run) and 800 mL FW (TCOD of FW was 40 g/L)
		Org-N	Repeated batch	1000	9.0 ± 0.1	--	R1: 200 mL SR and 800 mL (Mixture of FW and autoclaved WAS) R2 -R8: 200 mL (substrate from last Run) and 80% (Mixture of FW and autoclaved WAS) (TCOD of FW and autoclaved WAS mixture was 40 g/L)
		Am-N	Repeated batch	1000	9.0 ± 0.1	NH_4^+-N 300 mg/L	R1: 200 mL SR and 800 mL (FW and ammonium) R2 -R8: 200 mL (substrate from last Run) and 800 mL (FW and ammonium) (TCOD of FW was 40 g/L)
Test 5 ^{15}N isotope tracing	Figure 4b and Figure S10	$^{15}NH_4$-R	Batch	500	9.0 ± 0.1	$^{15}NH_4^+$-N 300 mg/L	50 mL (substrate from Am-N) and 450 mL (FW and ammonium) (TCOD of FW was 40 g/L)
Test 6 Interaction of pyruvate and ammonium	Figure 5 Table S7	NH_4-R	Batch	220	7.0 ± 0.1	NH_4^+-N 300 mg/L	10 mL (substrate from Am-N) and 200 mL (ammonium)
		Py-R	Batch	220	7.0 ± 0.1	Pyruvate 1500 mg/L	10 mL (substrate from Am-N) and 200 mL (Pyruvate)
		$PyNH_4$-R	Batch	220	7.0 ± 0.1	Pyruvate 1500 mg/L, NH_4^+-N 300 mg/L	10 mL (substrate from Am-N) and 200 mL (ammonium and pyruvate)

Table S2

Statistical Analysis of L-, D-, and total lactic acid production and OA of L-lactic acid in repeated batch fermentation in Ctrl, Org-N and Am-N.

Reactor	stable cycle	T-lactic acid		L-lactic acid		D-lactic acid		OA of L-lactic acid	
		F	***p-value***	**F**	***p-value***	**F**	***p-value***	**F**	***p-value***
Ctrl	1~8	2.396	0.052	2.396	0.052	2.405	0.051	25.605	1.16E-09
	2~8	2.546	0.052	2.546	0.052	2.339	0.069	30.105	2.85E-09
	3~8	0.782	0.575	0.782	0.575	1.371	0.281	5.479	0.003
	4~8	0.887	**0.495**	0.887	**0.495**	1.238	0.337	2.987	**0.053**
Org-N	1~7	2.211	0.083	2.211	0.083	6.790	4.14E-04	10.906	1.54E-05
	1~6	1.635	**0.201**	1.635	**0.201**	4.793	0.006	12.720	2.19E-05
Am-N	1~7	0.537	0.774	0.537	0.774	5.024	0.002	8.178	1.22E-04
	1~8	0.638	**0.720**	0.638	**0.720**	6.845	1.60E-04	15.556	1.61E-07

Table S3

The productivity of L-, D- and total lactic acid in Ctrl, Org-N and Am-N.

Reactor	The productive rate of L-lactic acid (g COD/L·d)		The productive rate of D-lactic acid (g COD/L·d)		The productive rate of total-lactic acid (g COD/L·d)	
	k [a]	***R²***	***k***	***R²***	***k***	***R²***
Ctrl	1.34 ± 0.29	0.9955	1.0 ± 0.22	0.9996	2.34 ± 0.30	0.9991
Org-N	4.58 ± 0.58	0.9967	1.74 ± 0.42	0.9951	6.32 ± 0.61	0.9963
Am-N	4.69 ± 0.31	0.9879	0.91 ± 0.28	0.9986	5.60 ± 0.80	0.9906

[a] *k* was the first order reaction rate constant based on the average of L-, D- and total lactic acid variations in the repeated batch fermentation.

Table S4

Statistical Analysis of ΔS_{COD}, Protease and α-glucosidase.

	Items	ΔSCOD	Protease	α-glucosidase
One-Way ANOVA	Between Groups	0.038	0.000	0.000
Post Hoc tests	Ctrl *vs* Org-N	0.208	0.000	0.000
	Ctrl *vs* Am-N	0.042	0.682	0.000
	Am-N *vs* Org-N	1.000	0.000	0.000

Table S5

C/N ratio in different substrates from Ctrl, Org-N and Am-N reactors.

Reactors	C/N
Ctrl	31.06 ± 4.18
Org-N	16.04 ± 2.60
Am-N	24.61 ± 1.83

Table S6

Community richness and diversity in the samples from different reactors.

Reactor	Chao1 [a]	ACE [b]	Shannon [c]	Simpson [d]
SR	500.92	497.05	4.72	0.88
Ctrl	280.31 ± 27.99	291.27 ± 33.96	2.78 ± 0.06	0.61 ± 0.00
Org-N	429.23 ± 72.51	436.59 ± 71.57	4.13 ± 0.11	0.82 ± 0.04
Am-N	296.28 ± 32.58	296.74 ± 31.7	3.68 ± 0.59	0.81 ± 0.07

[a] Chao1 richness estimator: the total number of OTUs estimated by infinite sampling. A higher number indicates higher richness.
[b] ACE richness estimator: the total number of OTUs estimated by infinite sampling. A higher number represents higher richness
[c] Shannon diversity index: an index to characterize species diversity. A higher value represents more diversity.
[d] Simpson diversity index: an index to characterize species diversity. A higher value represents more diversity.
Community diversity increased in the order of Ctrl < Am-N < Org-N < SR, thus, adding nitrogen substrates increased microbial diversity.

Table S7

Electron balance calculation between oxidation of ammonium into nitrate and reduction of pyruvate into lactate in $PyNH_4$-R and Am-N.[a]

Reactors	Fed with pyruvate and ammonium ($PyNH_4$-R)			Fed with food waste and ammonium (Am-N)		
	Reactant		Product	Reactant		Product
Donor	NH_4^+-N	→	NO_3^--N	NH_4^+-N	→	NO_3-N
	20.23 mM		19.82 mM	20.32 mM		21.28 mM
Acceptor	Pyruvate	→	Lactate	Pyruvate	→	Lactate
	32.17 mM		21.27 mM	NA[b]		510 mM
Electron balance	Donor (19.89mM) ≈ Acceptor (21.27 mM)			Donor (21.28mM) << Acceptor (510mM)		

[a] Based on the equations for oxidation of ammonium (E=-0.44V) and reduction of pyruvate (E=-0.19V), the spontaneous reaction ($\Delta G = -nF\Delta E = -8\times96485\times(-0.19+0.44) = -192.97$ KJ/mol < 0) was obtained in which NH_4^+-N may act as the electron donor while pyruvic acid may act as the electron acceptor. Electron balances were calculated based on two cases: $PyNH_4$-R (NH_4^+-N and pyruvate in Figure 5) and Am-N (NH_4^+-N and food waste in Figure 1). In each case, donated and accepted electrons were calculated based by either the reactant (ammonium and pyruvate) or the product (nitrate and lactate). The calculations were detailed in Supplementary material.

[b] NA (not available), pyruvate is an intermediate metabolite in food waste fermentation (Figure S7), which is not accurate for calculation in Am-N.

Table S8

ORP variation in synthetic media after ammonium, lactic acid and/or acetic acid addition.

Anaerobic synthetic media	Addition and dosage	ORP (mV)[a]
Deoxygenated distilled water + NH_4^+-N (pH was adjusted to 9.0 after ammonium addition)	NH_4^+-N 0 mg/L	-101
	NH_4^+-N 100 mg/L	-99
	NH_4^+-N 200 mg/L	-90
	NH_4^+-N 300 mg/L	-81
	NH_4^+-N 400 mg/L	-80
	NH_4^+-N 500 mg/L	-80
	NH_4^+-N 1000 mg/L	-77
Deoxygenated distilled water + NH_4^+-N (300 mg/L) + organic acids (in the left) (pH was adjusted to 9.0 after lactic or acetic acid addition)	Blank	-81
	lactic acid 10 g/L	-8
	lactic acid 20 g/L	-10
	acetic acid 4 g/L	-27
	acetic acid 8 g/L	-23
	lactic acid 10 g/L + acetic acid 4 g/L	-23
	lactic acid 20 g/L + acetic acid 8 g/L	-19

[a] ORP was tested after ultrasonic degas and N_2 blowing for 15min to evacuate O_2 from liquid and headspace.

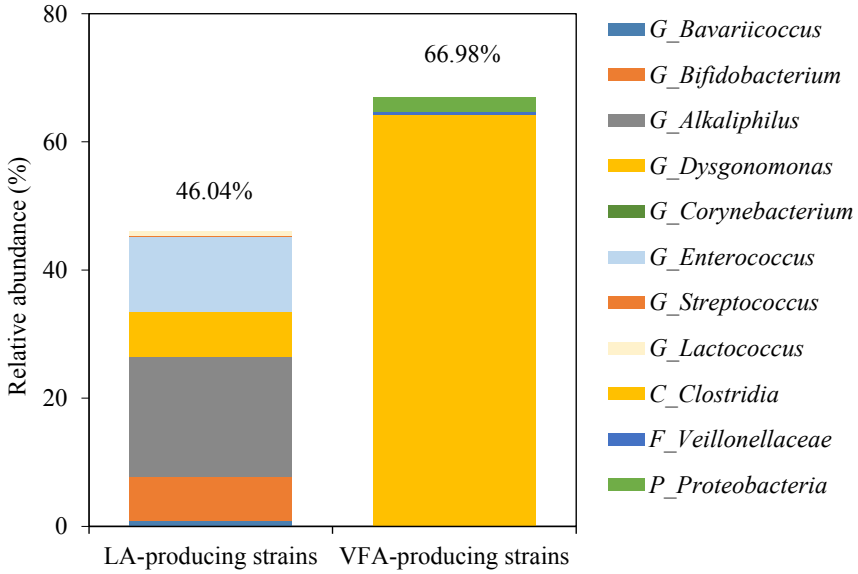

141

142 **Figure S1.** Relative abundance of VFA-producing strains and LA-producing bacteria during the repeated batch

143 fermentation of FW and WAS.

144

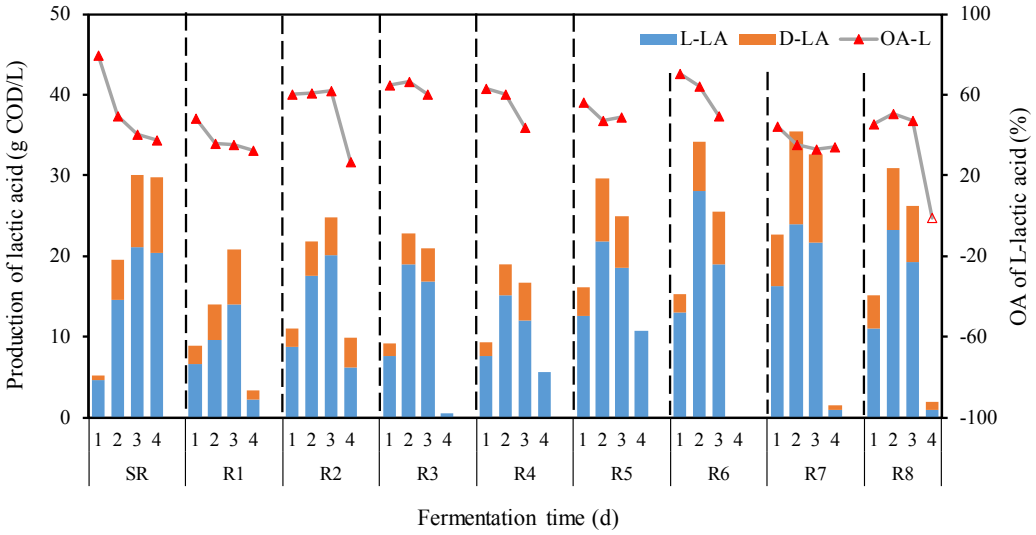

145

146 **Figure S2.** The yields of L- and D-lactic acid and the OA of L-lactic acid through repeated batch fermentation of FW

147 and WAS.

148

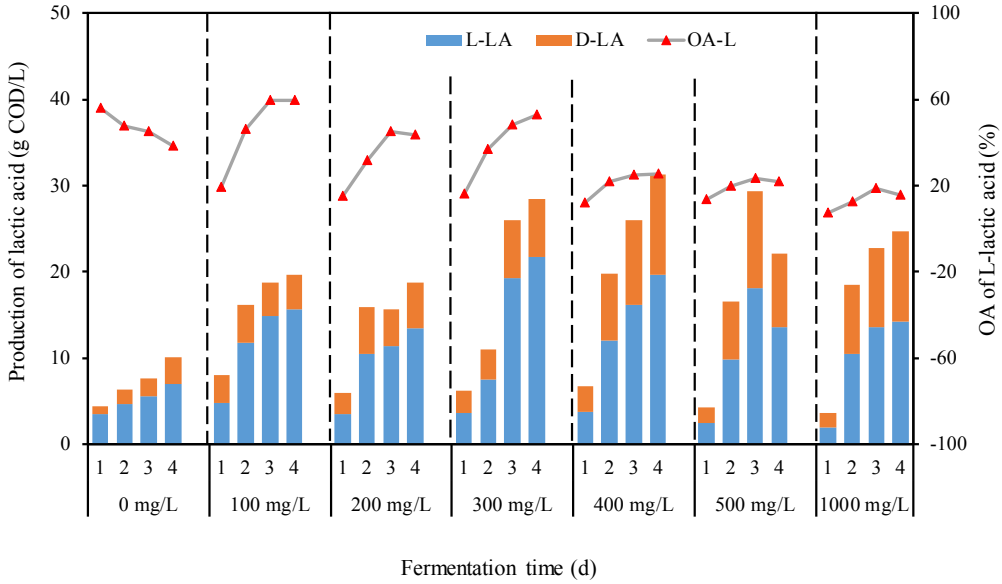

Figure S3. The yields of L- and D- lactic acid and the OA of L-lactic acid at different NH_4^+-N dosages.

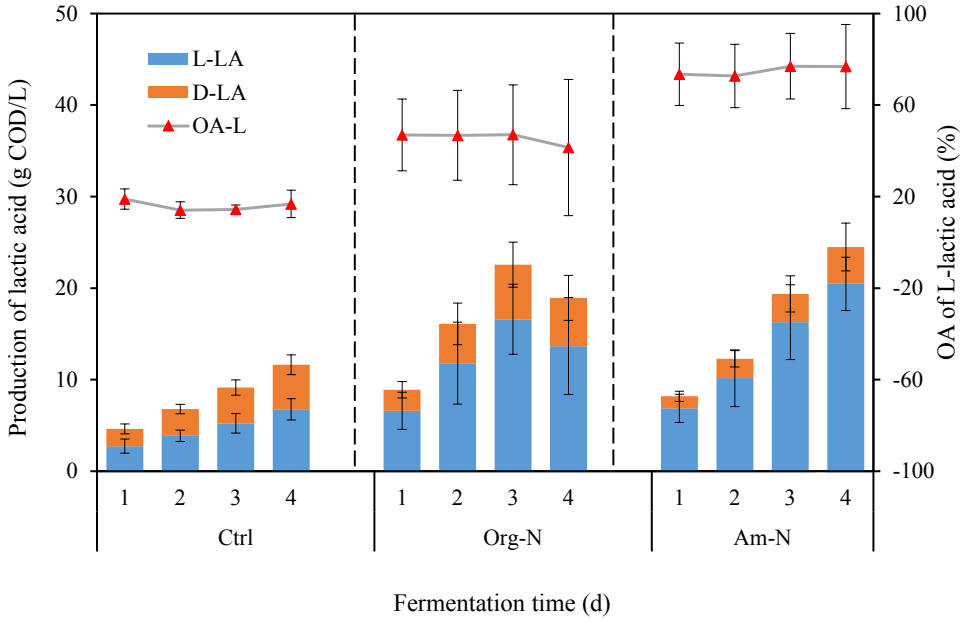

Figure S4. The average yield of L- and D- lactic acid and OA of L-lactic acid from eight cycles of the repeated batch fermentation. Error bars represent standard errors (n=8).

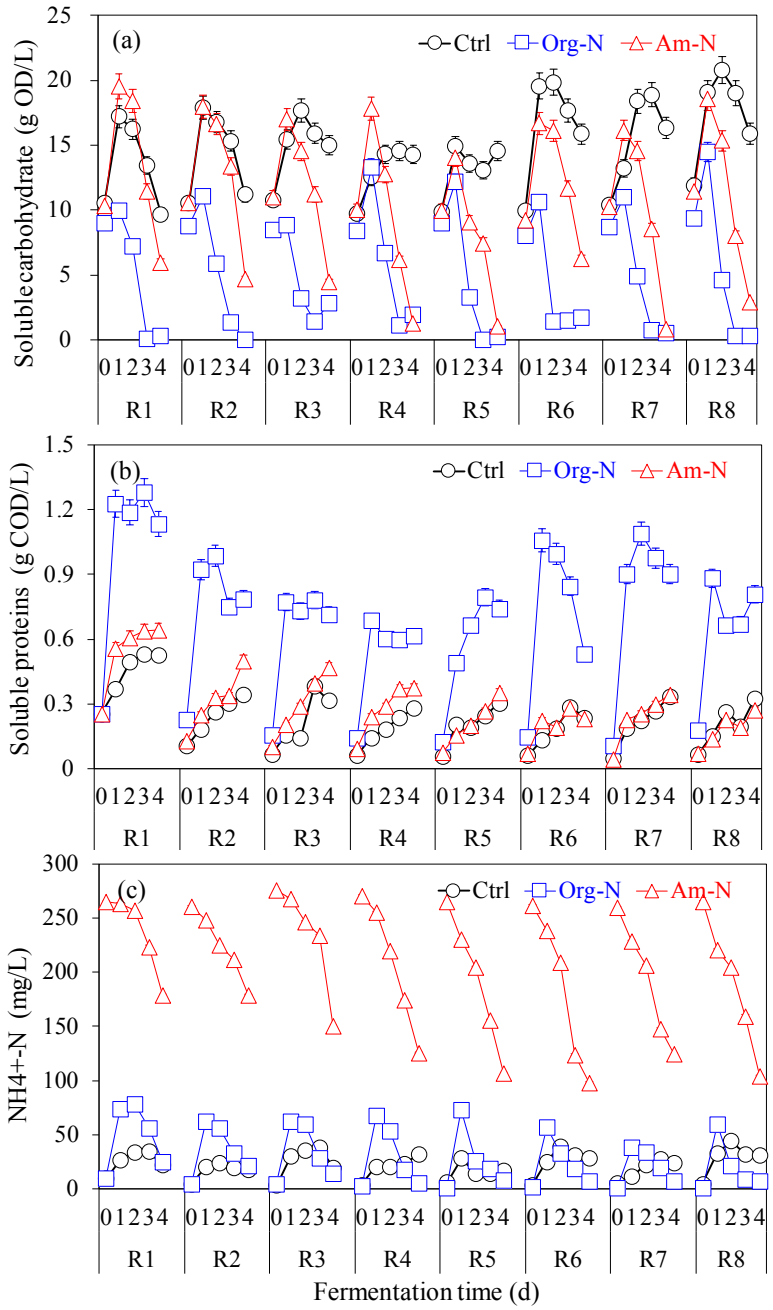

Figure S5. The variation of (a) soluble carbohydrate, (b) proteins, and (c) NH_4^+-N during repeated batch fermentation in three reactors. Error bars represent standard errors (n = 3). It should be emphasized that after 4 days of fermentation, 83.18 ± 9.82% of carbohydrate was degraded in Am-N (Figure S5a), suggesting that although the hydrolysis rate was lower in Am-N compared to Org-N, the weak hydrolysis did not affect the utilization of carbohydrate. The concentration of protein decreased in Org-N from (956.97 ± 175.01 mg COD/L in average) to (756.39± 188.57 mg COD/L) during the repeated batch fermentation, whereas it was slowly edging upward from (166.11 ± 24.25 mg COD/L) to (305.75 ± 33.87 mg COD/L) in Ctrl and (206.21 ± 39.58 mg COD/L) to (363.62 ± 89.95 mg COD/L) in Am-N (Figure S5b).

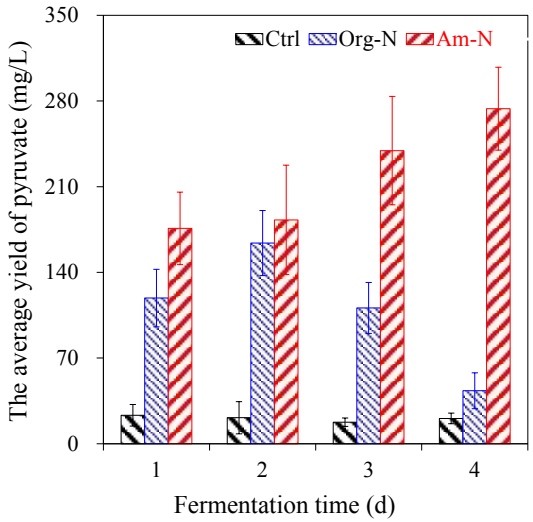

164

165 **Figure S6.** The average yield of pyruvate in eight cycles of the repeated batch fermentation from three reactors.

166

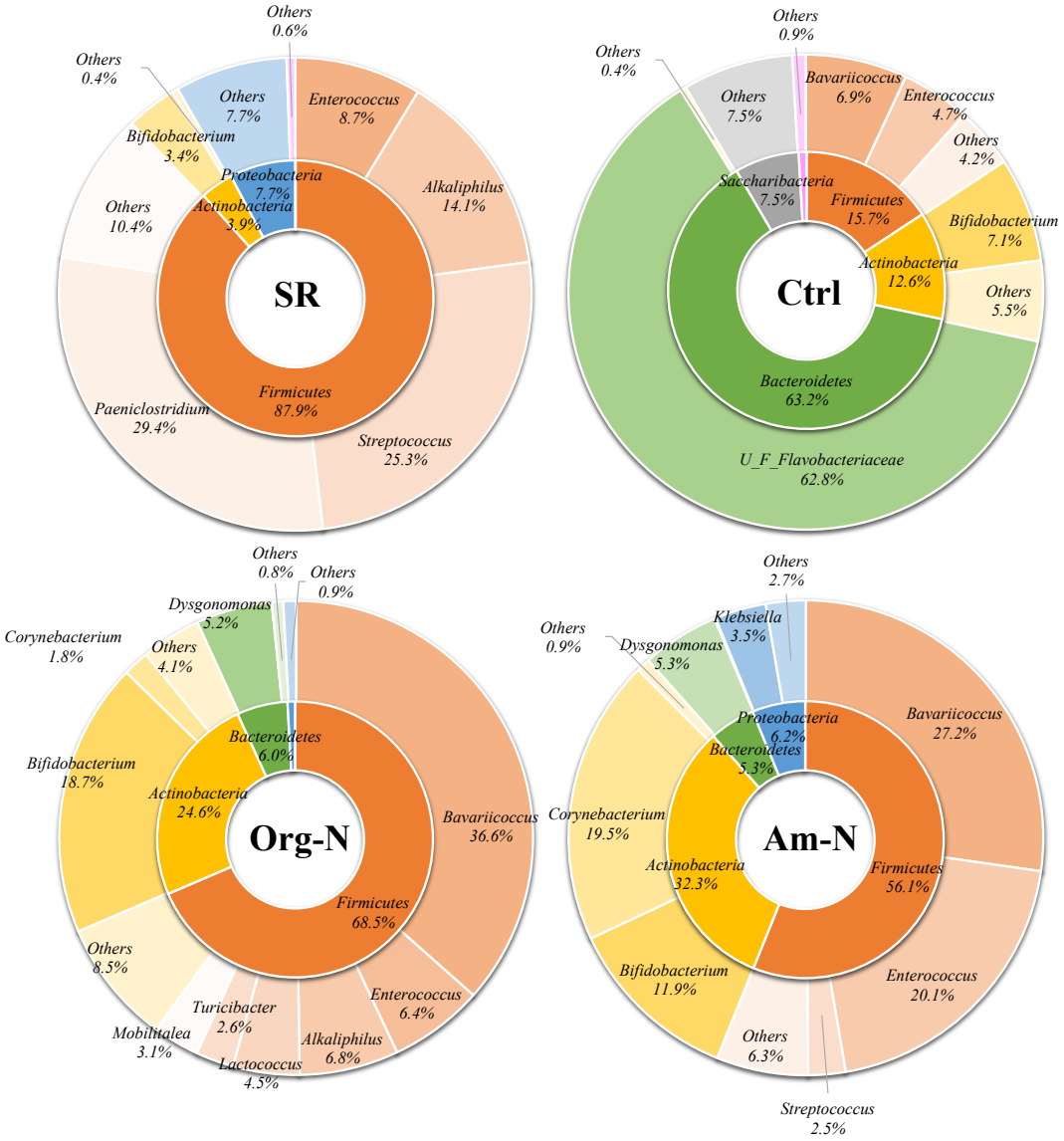

Figure S7. Relative abundance of bacteria on phylum (inside) and genus (outside) levels. The bacteria with < 2% abundance are integrated as others. At the phylum level, bacterial 16S rRNA in all samples were dominated by populations related to *Firmicutes*, *Actinobacteria*, *Bacteroidetes* and *Proteobacteria*, which were capable of converting complex organic compounds to LA and VFAs in anaerobic conditions. The dominant phylum in Ctrl was *Bacteroidetes* (63.2%), whereas *Firmicutes* and *Actinobacteria* were dominant in SR (91.7%), Am-N (88.4%), and Org-N (93.2%).

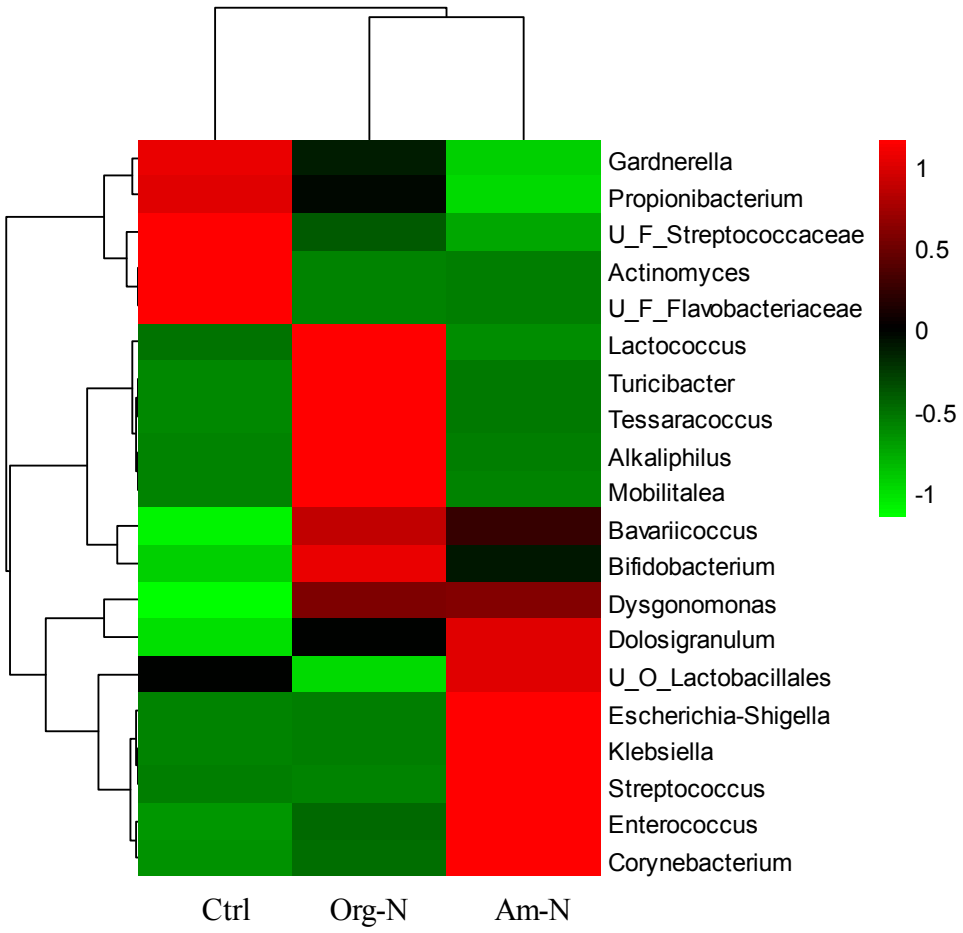

175

176 **Figure S8.** Heat map of 10 most abundant genera in each sample determined by 16s rRNA sequencing.

177

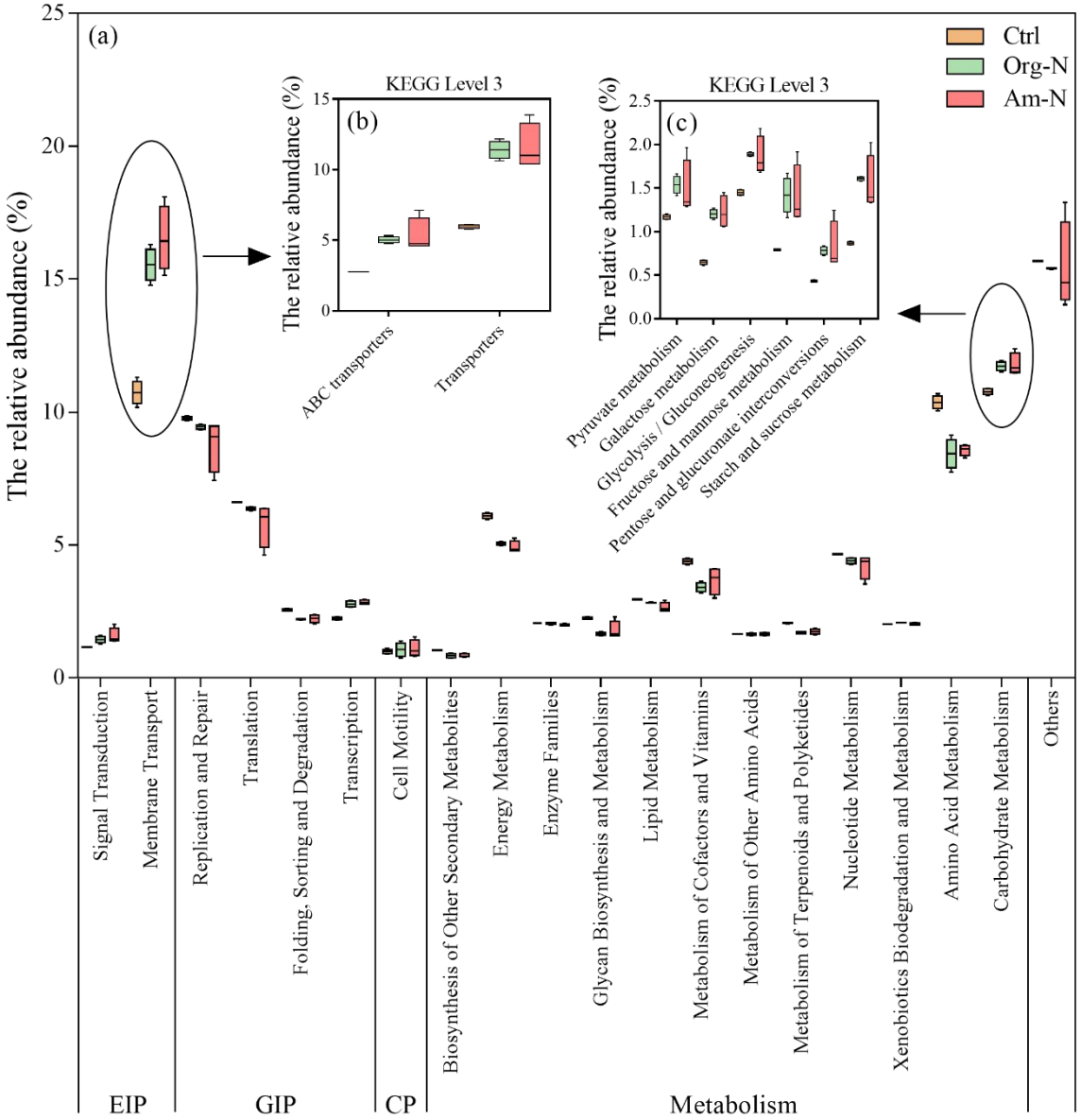

Figure S9. Abundance of functional genes based on KEGG datasets in the repeated batch fermentation of Ctrl, Org-N, and Am-N. (a) The abundance of functional genes at level two in Environmental Information Processing (EIP), Genetic Information Processing (GIP), Cellular Processes (CP), Metabolism, and Others contents; (b) details for membrane transports at level three; and (c) details for carbohydrate metabolism at level three.

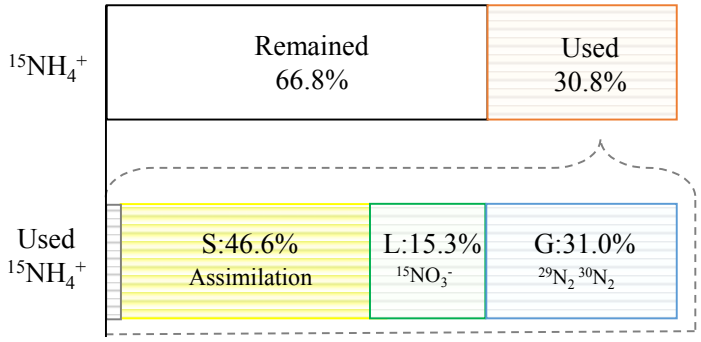

Figure S10. The ammonia transformation based on ^{15}N isotope tracing technique. S: Solid; L: Liquid; and G: Gas.

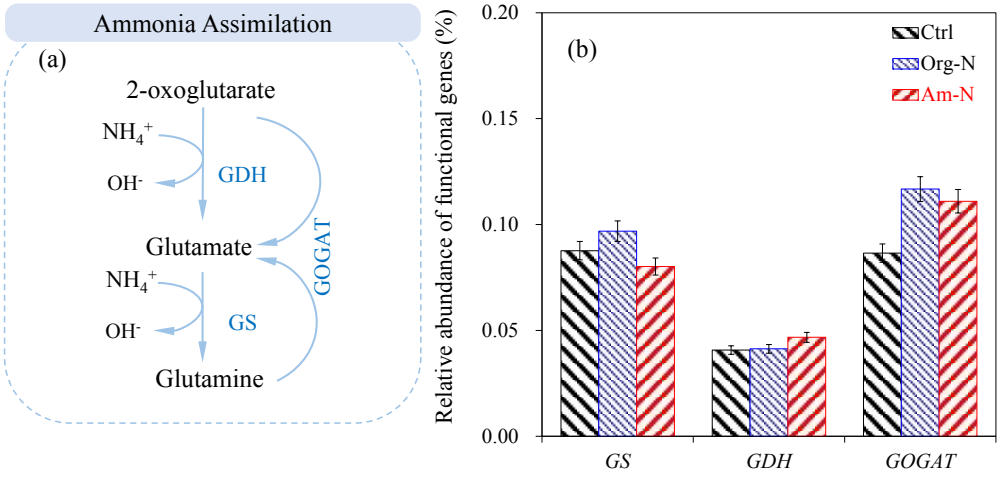

Figure S11. (a) Ammonia depletion through biological ammonia assimilation and (b) the relative abundance of functional genes forecasted based on KEEG pathway database. Error bars represent standard errors (n=3). In the ammonia assimilation, glutamate dehydrogenase (GDH) catalyzes the conversion of 2-oxoglutarate utilizing ammonia as a substrate. A secondary pathway involves glutamine synthetase (GS), which synthesizes glutamine from glutamate and ammonia with a glutamate synthase (GOGAT).

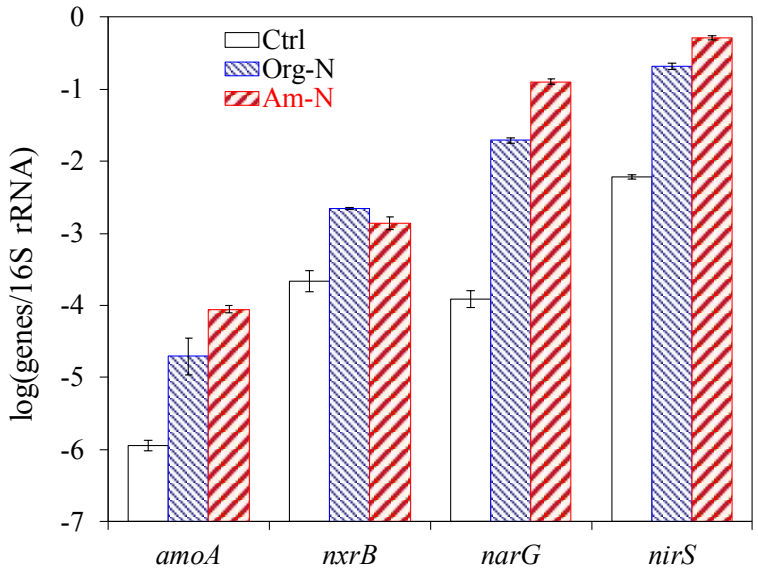

Figure S12. qPCR for ammonia oxidation related genes (*amoA* and *nxrB*) and denitrification related genes (*narG* and *nirS*).

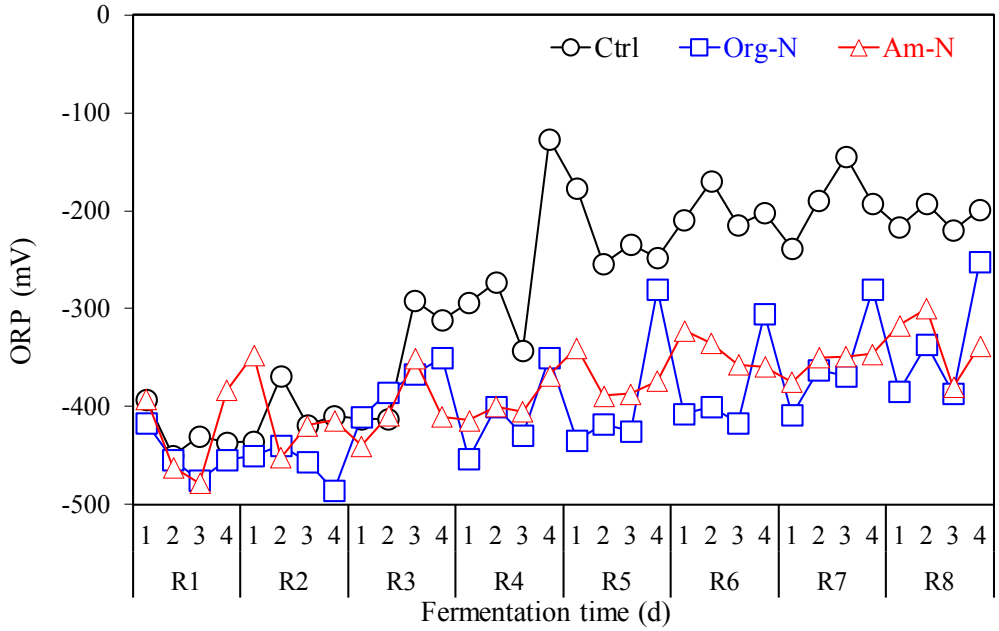

Figure S13. ORP in eight cycles of the repeated batch fermentation in Ctrl, Org-N and Am-N. ORP was around -380 ± 42 mV during the entire fermentation period, which guaranteed the benign reducing environments for L-LA production.

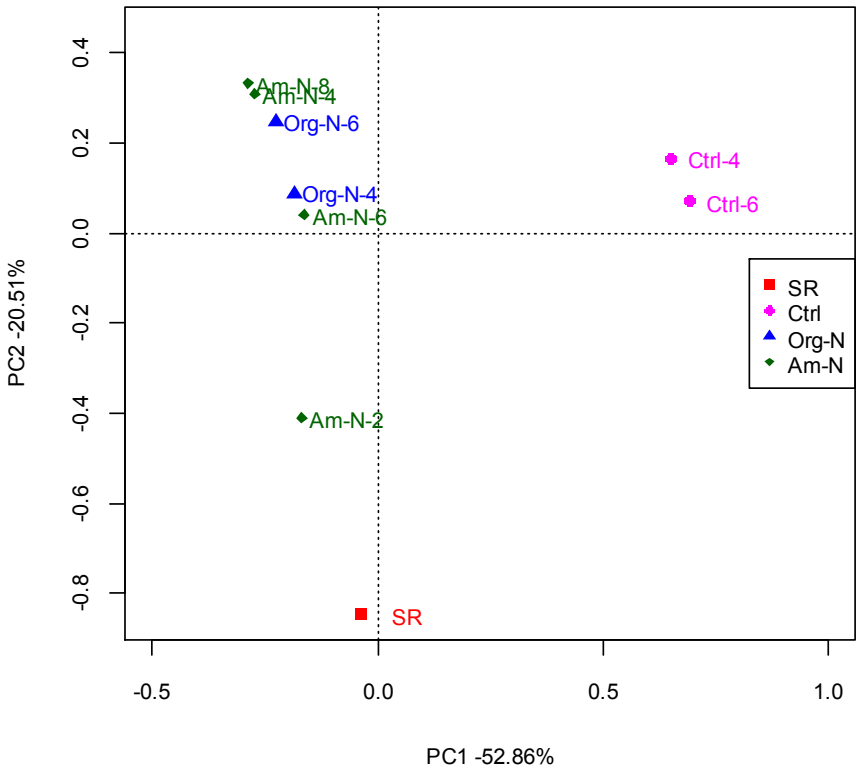

Figure S14. Principal component analysis (PCA) results of bacterial community fetched from different reactors based on OTU (3 % distance). The shared OTUs were analyzed at the phylum level. Principal components (PC) 1 and 2 explained 52.86 and 20.51%, respectively, of the total changes of bacterial community structure. The reactors with or without the supply of nitrogen source were correlated with the PC1 vector, whereas the fermentation cycles were correlated with the PC2 vector. Microbial community structure was primarily affected by the feed substrates (Ctrl versus Org-N or Am-N) since principal component 1 explained 52.86% of total bacterial community variations based on PCA analysis.

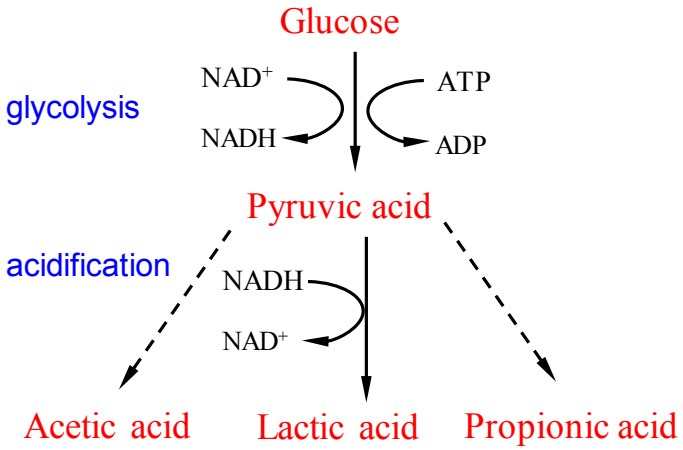

Figure S15. Regeneration of NADH in glycolysis and metabolic pathway of lactate production.